

In-plane Magnetic Anisotropy Generated by Quantum Zero-point Fluctuations in a Tetragonal Quantum Antiferromagnet Bi_2CuO_4

Bo Yuan,¹ Nicholas P. Butch,² Guangyong Xu,² and Young-June Kim¹

¹*Department of Physics, University of Toronto, Toronto, Ontario, Canada, M5S 1A7*

²*NIST Center for Neutron Research, National Institute of Standards and Technology, Gaithersburg, Maryland 20899, USA*

(Dated: November 25, 2021)

We carried out inelastic neutron scattering measurements to study low energy spin dynamics of a tetragonal quantum magnet Bi_2CuO_4 . Unlike other previously studied cuprates, its unique magnetic lattice gives rise to an accidental in-plane spin rotational symmetry, not present in the microscopic Hamiltonian. We demonstrate that this accidental symmetry is removed by an in-plane magnetic anisotropy produced by quantum zero-point fluctuations using spin-wave theory calculations. In addition, we find that the size of the in-plane anisotropy agrees quantitatively with the spin-flop transition field of ~ 0.4 T, revealed by our neutron scattering measurements. The spin Hamiltonian used for the calculation is determined independently from the dispersion of the out-of-plane mode. Our results show that a rare display of quantum fluctuations in a three-dimensional quantum magnet is found in Bi_2CuO_4 .

PACS numbers:

Determination of the ground state of a magnetic system is one of the central goals in the study of magnetism. In most cases, it is sufficient to treat the problem classically by minimizing the energy while treating the spins as classical vectors; quantum zero point fluctuation (QZPF) in these cases is responsible for only quantitative renormalization of the ground state properties from their classical values [1]. However, QZPF can play a decisive role in the determination of ground state in systems with lower spatial dimensions or in the presence of magnetic frustration such as quantum spin liquids [2]. While magnetic order is destroyed by QZPF in quantum spin liquids, there exists another scenario where the QZPF actually stabilizes the order. This arises when there is an accidental degeneracy within a continuous manifold of states on a classical level. This could happen in systems with high crystalline symmetries where anisotropic terms in the microscopic Hamiltonian cancel on average, leaving the mean-field energy functional with a higher symmetry than that of the actual Hamiltonian. Since this degeneracy is not protected by symmetry, it can be removed by an anisotropy generated by QZPF, which selects and stabilizes the correct ground state[3–5]. This was recently demonstrated in a three-dimensional frustrated magnet with pyrochlore structure $\text{Er}_2\text{Ti}_2\text{O}_7$ [6, 7].

Despite extensive theoretical efforts, finding clear evidence for anisotropy generated by QZPF is challenging because small symmetry-allowed perturbations tend to be present in real materials and compete with the QZPF effect. Although this phenomena has long been proposed for layered cuprates with a tetragonal lattice structure and an in-plane magnetic order[8–10], a clear demonstration of an anisotropy generated by QZPF within the easy (ab) plane has remained elusive. The presence of an orthorhombic distortion or a second interpenetrating square lattice provides additional small per-

turbations that compete with the QZPF in La_2CuO_4 [11–14] and $\text{Sr}_2\text{Cu}_3\text{O}_4\text{Cl}_2$ [15–17], respectively. Although $\text{Sr}_2\text{CuO}_2\text{Cl}_2$ does not suffer from the above problems, the relative displacement between neighbouring CuO_2 layers lowers the symmetry of the mean-field energy by allowing inter-planar dipolar and pseudo-dipolar interactions[10], which is of the same order of magnitude as the anisotropy generated by QZPF[15].

As shown in Fig. 1, the magnetic Cu^{2+} ions in Bi_2CuO_4 are arranged in a square lattice stacked directly on top of each other. Structurally, it is similar to undoped $\text{YBa}_2\text{Cu}_3\text{O}_6$, where QZPF has also been considered[8] but has never been directly observed[18]. Its lattice structure remains tetragonal down to the lowest temperature[19]. Below $T_N \sim 50$ K, spins confined in the ab plane[20] order ferromagnetically along c and antiferromagnetically in the ab plane as shown in Fig. 1[19, 21–23]. By virtue of the four-fold symmetry, the crystal is invariant under a $\pi/2$ rotation. Because of the simple magnetic lattice with ferromagnetic chains arranged in a square lattice, this operation moves atoms only within its own sub-lattice for Bi_2CuO_4 , unlike other tetragonal cuprates such as $\text{Sr}_2\text{CuO}_2\text{Cl}_2$. The four-fold *structural* symmetry, which moves both atoms as well as rotates spins, is therefore equivalent to a four-fold *spin – rotational* symmetry. The latter guarantees any in-plane anisotropy to cancel on the mean-field level (See Supplementary Materials for more details), thus ruling out the anisotropy terms considered for $\text{Sr}_2\text{CuO}_2\text{Cl}_2$ and $\text{Sr}_2\text{Cu}_3\text{O}_4\text{Cl}_2$ as alternative explanations for the observed anisotropy.

In this letter, we report our neutron scattering study of spin dynamics along with spin-wave theory calculations to show that the in-plane anisotropy in Bi_2CuO_4 is generated by QZPF. Existence of the in-plane anisotropy is unambiguously demonstrated by the observation of a spin-

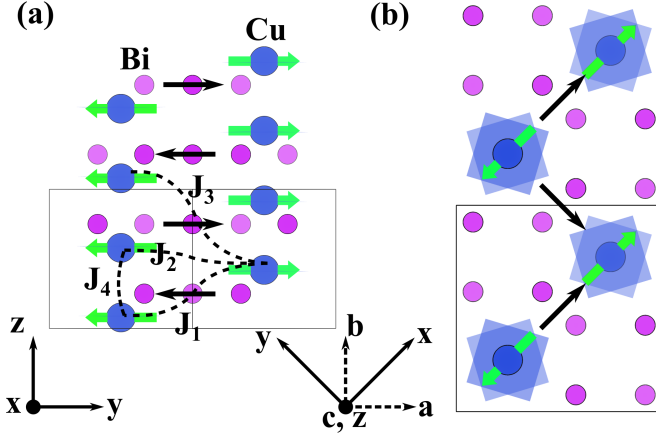


FIG. 1: (a) Structure of Bi_2CuO_4 projected onto the yz plane showing two unit cells along z . z coincides with c while x and y are rotated 45° with respect to crystallographic a and b . Copper and bismuth ions are shown by blue and purple spheres. The CuO_4 squares are shaded in blue. Oxygen ions are not shown here (See Supplementary Materials for structure with oxygen ions). Dominant Heisenberg interactions $J_1 - J_4$ considered in the spin wave calculation are indicated by dashed lines. (b) Structure of Bi_2CuO_4 projected onto the ab plane. DM vectors for the exchange path J_1 (\vec{D}_1) as well as symmetry related bonds are shown with black arrows. Green arrows indicate directions of ordered Cu moments.

flop transition within the easy plane at $H_c \sim 0.4\text{T}$, which is then *quantitatively* explained with the anisotropy generated by QZPF from our spin wave theory calculation. The spin Hamiltonian used for the calculation includes both the antisymmetric (Dzyaloshinskii-Moriya, or DM) and symmetric anisotropic interactions, and is *independently* determined by fitting the out-of-plane magnon mode. Our results therefore establish that Bi_2CuO_4 is an example in which magnetic properties are modified on a qualitative level by QZPF.

Bi_2CuO_4 single crystal (4.35g) used for neutron scattering measurements was grown using the floating zone technique. Time-of-flight neutron scattering measurements were carried out using the Disk Chopper Spectrometer (DCS) at the NIST Center for Neutron Research (NCNR). Two incident energies of $E_i = 4.9\text{meV}$ and $E_i = 2.3\text{meV}$ were used with an energy resolution of $\sim 0.18\text{meV}$ and $\sim 0.06\text{meV}$ respectively. Triple axis measurements were carried out using Spin Polarized Inelastic Neutron Spectrometer (SPINS) at the NCNR with a fixed final energy $E_f = 5\text{meV}$. A vertically focussing pyrolytic graphite (PG) monochromator, flat PG analyzer and a Be filter was used to select incident and final energies. A collimation setting of guide-open- 80° -open was used to achieve an energy resolution of $\sim 0.3\text{meV}$. For all measurements, the crystal was aligned with the ac -plane in the scattering plane. A 10T vertical field superconducting magnet was used in both measurements to apply a field along b axis. The sample temperature was kept at

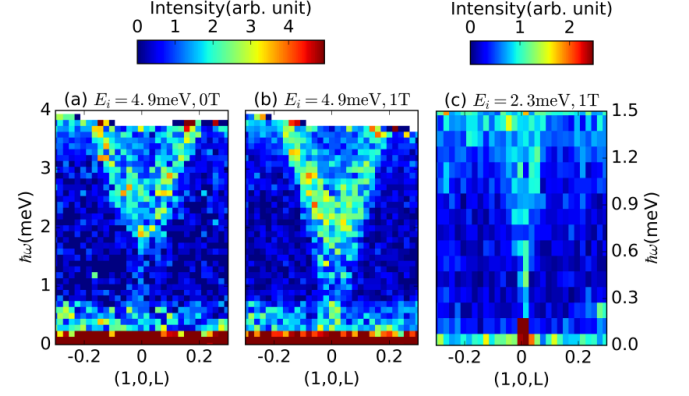


FIG. 2: Neutron intensity near $(1,0,0)$ magnetic Bragg peak as a function of momentum transfers along $(1,0,L)$ (in reciprocal lattice units) and energy transfer ($\hbar\omega$). Neutrons with incident energy $E_i = 4.9\text{meV}$ were used for (a) and (b), which was obtained with applied fields of 0T and 1T along b . (c) was obtained using $E_i = 2.3\text{meV}$ and a field of 1T along b .

$\sim 1.5\text{K}$ for all measurements.

Scattered neutron intensity obtained with incident energy $E_i = 4.9\text{meV}$ near the magnetic Bragg peak position $(1,0,0)$ is shown in Fig. 2(a)-(b) as a function of momentum along L and energy transfer $\hbar\omega$. A clear dispersive magnon mode with $\sim 2\text{meV}$ gap can be resolved in Fig. 2(a) at zero field. This gap was also observed in earlier neutron experiment [24]. What is not apparent in this plot is the existence of another mode with acoustic-like dispersion relation. We found that these two modes can be distinguished clearly when magnetic field is applied as shown below.

When a 1T field was applied along the b axis, the intensity of the $\sim 2\text{meV}$ gapped mode remains more or less unchanged, whereas the spectrum below this mode intensifies as shown in Fig. 2(b). This clearly indicates that in addition to the gapped mode, there is another magnon mode whose intensity is enhanced by a magnetic field along b . The second mode is also highly dispersive and becomes almost degenerate with the first mode away from the antiferromagnetic zone center. In contrast to the gapped mode, this mode is apparently gapless and its intensity extends down to the incoherent background level. The gap cannot be resolved even in a high resolution measurement using incident neutron energy $E_i = 2.3\text{meV}$ as shown in Fig. 2(c). The gapless and gapped magnon mode come from spin fluctuation within and out of the ab plane, which is consistent with easy-plane anisotropy in Bi_2CuO_4 .

To track intensity change of the two modes as a function of applied field, a triple axis measurement was carried out at fixed $\mathbf{Q} = (1,0,0)$. Neutron intensity as a function of energy transfers are shown in Fig. 3(a) for differ-

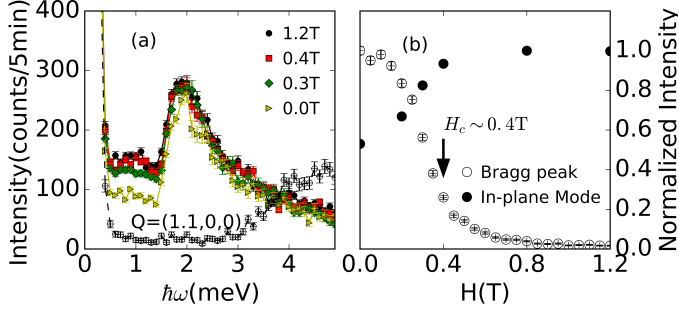


FIG. 3: (a) Constant- \mathbf{Q} scan at $\mathbf{Q}=(1,0,0)$ with different fields (0T-1.2T) along b . Open circle in the main plot is a scan at $\mathbf{Q}=(1.1,0,0)$ at zero field, which is used as non-magnetic background for energy transfer $0.5\text{meV} \lesssim \hbar\omega \lesssim 3\text{meV}$. Error bar on each data point represents one standard deviation. (b) Field dependence of (1,0,0) magnetic Bragg peak intensity (open circle) and intensity of the in-plane magnon mode (solid circle). Intensity of the in-plane magnon mode is obtained by integrating the constant- \mathbf{Q} scan at (1,0,0) from 0.5meV to 1.5meV after subtracting the background at (1.1,0,0) within the same energy range. Intensity of magnetic Bragg peak and gapless mode have been normalized with respect to the values at 0T and 1.2T respectively.

ent fields. The peak at $\sim 2\text{meV}$ in all constant- \mathbf{Q} scans corresponds to the gapped out-of-plane magnon mode shown in Fig. 2(a)-(b). Clearly, intensity of this mode is almost independent of applied field. We also plot the scan at $\mathbf{Q}=(1.1,0,0)$ obtained at zero field in Fig. 3(a) with open circles. Since the magnon has fairly steep dispersion, at this \mathbf{Q} it has dispersed to higher energy ($\hbar\omega > 3\text{meV}$) and the small residual intensity for energy transfers $0.5\text{meV} \lesssim \hbar\omega \lesssim 3\text{meV}$ can be taken as the background. Compared to the $\mathbf{Q}=(1.1,0,0)$ data, the scan at $\mathbf{Q}=(1,0,0)$ at zero field clearly shows additional inelastic intensity below the $\sim 2\text{meV}$ peak that extends down to elastic region. This intensity comes from the gapless in-plane magnon mode and grows with increasing field. To obtain a quantitative measure of the in-plane magnon mode intensity, the background at $\mathbf{Q}=(1.1,0,0)$ was first subtracted from the scan at $\mathbf{Q}=(1,0,0)$, and then the intensity from 0.5meV to 1.5meV was integrated. The integrated intensity is plotted as a function of applied field strength in Fig. 3(b) (solid circle). One can observe that the in-plane mode intensity in this energy range almost doubles from 0T to $\sim 0.4\text{T}$ and then stays the same beyond this field. Also shown in Fig. 3(b) is intensity of the magnetic Bragg peak at $\mathbf{Q}=(1,0,0)$ represented by open circles, which is completely suppressed as the intensity of the in-plane mode reaches its maximum. Both the intensity of the in-plane mode and the (1,0,0) magnetic Bragg peak intensity changes most rapidly at $H_c \sim 0.4\text{T}$. It coincides with the metamagnetic transition observed in bulk magnetization studies, which was attributed to be a spin-flop transition[23]. As we will explain later, the

intensity change is entirely consistent with re-orientation of spins due to spin flop transition within the ab plane. If magnetic interactions are truly isotropic within the ab plane, spins can rotate freely and respond to even an infinitesimal field. Observation of a spin-flop transition at a finite field therefore directly indicates the existence of a small in-plane anisotropy.

To explain these observations, we carry out linear spin wave theory (LSWT) analysis. We have defined unit vectors \hat{x} , \hat{y} and \hat{z} in addition to the crystallographic a , b and c axes as shown in Fig. 1(b).

Magnetic interactions between $S = \frac{1}{2}$ spins on Cu^{2+} ions take the form:

$$J\vec{S}_1 \cdot \vec{S}_2 + \vec{D} \cdot (\vec{S}_1 \times \vec{S}_2) + \frac{|\vec{D}|^2}{4J} [2(\hat{d} \cdot \vec{S}_1)(\hat{d} \cdot \vec{S}_2) - \vec{S}_1 \cdot \vec{S}_2], \quad (1)$$

where $\hat{d} = \frac{\vec{D}}{|\vec{D}|}$. The first term is the usual Heisenberg exchange interaction. They are isotropic and hence do not contribute to magnetic anisotropy. The second and third terms are the DM and symmetric anisotropic exchange interactions (\vec{D} is called the DM vector). The last two terms introduced by Moriya[25] break full spin rotational symmetry and give rise to magnetic anisotropy as well as a gap in the magnon dispersion. Unlike Bi_2CuO_4 , we note that the anisotropic exchange terms in Eq. (1) are not allowed by symmetry in other layered cuprates where the super-exchange takes place along a 180° Cu-O-Cu bond. Much smaller perturbation arising from Coulomb exchange interaction was included to explain the magnetic anisotropy in the other cuprates[8]. In our calculation, we use the exchange interactions $J_1 - J_4$ (See Fig. 1) determined by Janson *et al*[27] $J_1=4.7\text{meV}$, $J_2=0.85\text{meV}$, $J_3=0.44\text{meV}$ and $J_4=0.88\text{meV}$. These values were determined by fitting to full magnon dispersion from earlier inelastic neutron scattering[24, 26] and by DFT calculation[27].

Since J_1 is the dominant Heisenberg interaction, we expect its anisotropic part \vec{D}_1 to be the leading anisotropic term. Anisotropic terms on the other bonds should be much smaller and therefore not included in the calculation. Symmetry analyses allow us to set $\vec{D}_1 = (D_1, 0, 0)$ and $\vec{D}_1 = (0, D_1, 0)$ for bonds directed along \hat{x} and \hat{y} , respectively (See Supplementary Materials). Resulting pattern of \vec{D}_1 vectors are shown as black arrows in Fig. 1. LSWT is carried out as a function of angle ϕ between the ordered moment direction and \hat{x} within the xy plane.

The out-of-plane magnon gap comes from symmetric anisotropic term in Eq. (1). To reproduce the observed gap size ($\Delta_\perp = 1.7\text{meV}$), we require $D_1 = 0.23J_1$. On the other hand, the in-plane magnon mode is gapless for all ϕ values within LSWT.

The absence of in-plane magnon gap as well as degeneracy of all ordering directions within the xy plane is a consequence of an accidental in-plane spin rotational

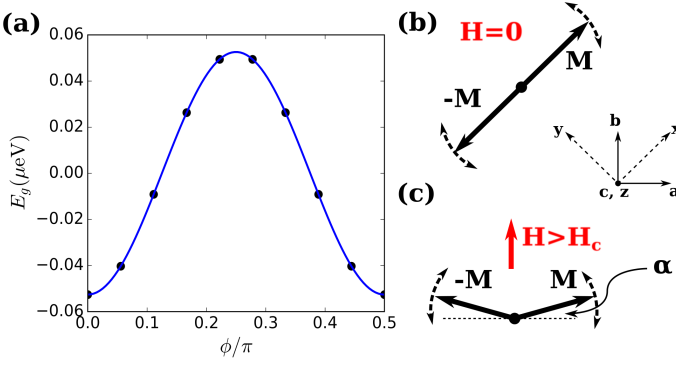


FIG. 4: (a) Ground state energy (E_g) per structural unit cell as a function of ordered moment direction ϕ after correcting for QZPF. E_g has been offset by a constant value -13.522045meV . Solid blue line is a fit to the ground state energy using $A \cos(4\phi)$ where $A = 0.0526\mu\text{eV}$. (b) Two sublattice magnetizations \vec{M} and $-\vec{M}$ for a domain with ordered moment parallel to \hat{x} at zero field. (c) When a field greater than critical field, H_c , is applied along b , a spin flop transition happens. The sublattice magnetizations \vec{M} and $-\vec{M}$ are re-oriented almost perpendicular to the field direction. α is the small canting of magnetic moments away from collinear configuration towards the field direction. The curved dashed arrows in (b) and (c) indicate directions of in-plane spin fluctuations.

symmetry of the mean-field free energy. This accidental symmetry is broken by including QZPF. The ground state energy for each structural unit cell as a function of ϕ is given by

$$E_g(\phi) = -6(J_1 + J_2 + J_3 - \frac{1}{2}J_4) + \frac{1}{2} \int_{FBZ} d\vec{k} \sum_{i=1}^4 \hbar \omega_{i,\vec{k}}(\phi),$$

if we include QZPF. The integral and sum are carried out over the first Brillouin zone and four magnon modes. The results are shown in Fig. 4(a) for $0 < \phi < \pi/2$. Ground state energy at other angles can be obtained by invoking the four-fold symmetry of Bi_2CuO_4 lattice. In Fig. 4(a), energy of the system is no longer independent of the ordered moment direction. It is the smallest for ordered moment along \hat{x} (and \hat{y}) and largest for moment along a (and b). The energy difference is given by $\Delta E_g \equiv E_g(\phi = 0) - E_g(\phi = \pi/4) \approx -0.1\mu\text{eV}$. Because of this anisotropy, the in-plane spin fluctuation should acquire a small gap. This could not be observed in Fig. 2 due to limited energy resolution. However, we will show below that this anisotropy explains the spin flop transition observed in Bi_2CuO_4 .

At zero field, ΔE_g pins the spins along \hat{x} or \hat{y} . In Fig. 4(b), we show a magnetic domain with two sublattice magnetizations, \vec{M} and $-\vec{M}$ parallel to \hat{x} (The analysis will not change for a domain with ordered moment along \hat{y}). When a magnetic field is applied along b , \vec{M} and $-\vec{M}$ are re-oriented almost perpendicular to

the field as in Fig. 4(c) if the Zeeman energy gain is sufficient to overcome the magnetic anisotropy. This leads to a spin-flop transition at a finite critical magnetic field, H_c . Microscopically, Zeeman energy comes from small canting of spins from collinear configuration towards the field direction (denoted by α in Fig. 4(c)). Classically, we can estimate its magnitude as

$$E_Z = -8(J_1 + J_2 + J_3 - \frac{1}{2}J_4)S^2 \cos(2\alpha) - 4HS \sin(\alpha).$$

Minimizing E_Z with respect to α gives $E_Z = -0.6H^2$ in μeV (H in Tesla). The spin flop transition should occur when $E_Z \sim \Delta E_g$, which gives $H_c^{theo} \sim 0.4\text{T}$.

Spin-flop transition within the ab plane explains the observed change in $(1,0,0)$ magnetic Bragg peak intensity as well as the intensity of in-plane mode shown in Fig. 3. At zero field, the ordered moment and in-plane magnetic fluctuation are parallel to \hat{x} and \hat{y} respectively as shown in Fig. 4(b). Neutron scattering is only sensitive to spin component along b , which is 45° from \hat{x} and \hat{y} , for scattering near $\mathbf{Q}=(1,0,0)$. Therefore, only half of the Bragg peak and in-plane magnon mode intensity at $(1,0,0)$ are detected at zero field. When field along b is greater than H_c of spin flop transition, all spins are re-oriented perpendicular to the field. The ordered moments are now almost parallel to a as depicted in Fig. 4(c) and hence do not contribute to Bragg peak intensity at $(1,0,0)$. On the other hand, in-plane spin fluctuation is now entirely along b . This maximizes the intensity of in-plane mode. Intensity of the in-plane mode for $H > H_c$ should be twice the intensity at zero field, in agreement with the integrated intensity at $H=0$ and $H=1.2\text{T}$ shown in Fig. 3. On the other hand, spin fluctuation along c is independent of spin orientations within ab plane, the out-of-plane mode should be unchanged across the spin flop transition. This is also consistent with our results in Fig. 3. The experimentally obtained value of critical field for the spin flop transition $H_c \sim 0.4\text{T}$ is in perfect agreement with the theoretically estimated critical field H_c^{theo} .

In conclusion, we have carried out high resolution inelastic neutron scattering to characterize the low energy spin dynamics in Bi_2CuO_4 . We note that nature of low energy magnetic excitations in Bi_2CuO_4 have been under constant debate. Early inelastic neutron scattering [24, 26, 28] found a large gap in the in-plane magnon dispersion. This contradicts the result of antiferromagnetic resonance (AFMR)[29], which found the in-plane mode to be gapless. Our results settled this long standing controversy by confirming the AFMR results. Moreover, by tracking the intensity of the in-plane magnon mode and magnetic Bragg peak, we directly observed a spin-flop transition at $\sim 0.4\text{T}$ when an in-plane magnetic field is applied. This clearly demonstrates the existence of a small in-plane magnetic anisotropy, which we have explained quantitatively by quantum zero-point fluctua-

tions. Our results establish Bi_2CuO_4 as a robust example exhibiting anisotropy generated by QZPF.

Work at the University of Toronto was supported by the Natural Science and Engineering Research Council (NSERC) of Canada. B.Y. acknowledges the support from NSERC Canada Graduate Scholarship-Doctoral (CGS-D). We acknowledge the support of the National Institute of Standards and Technology, U.S. Department of Commerce, in providing the neutron research facilities used in this work.

-
- [1] S. Chakravarty, B. I. Halperin, and D. R. Nelson, *Phys. Rev. B* **39**, 2344 (1989), URL <https://link.aps.org/doi/10.1103/PhysRevB.39.2344>.
 - [2] L. Balents, *Nature* **464**, 199 EP (2010), URL <https://doi.org/10.1038/nature08917>.
 - [3] C. L. Henley, *Phys. Rev. Lett.* **62**, 2056 (1989), URL <https://link.aps.org/doi/10.1103/PhysRevLett.62.2056>.
 - [4] E. Shender, *JETP* **56**, 178 (1982).
 - [5] Villain, J., Bidaux, R., Carton, J.-P., and Conte, R., *J. Phys. France* **41**, 1263 (1980), URL <https://doi.org/10.1051/jphys:0198000410110126300>.
 - [6] L. Savary, K. A. Ross, B. D. Gaulin, J. P. C. Ruff, and L. Balents, *Phys. Rev. Lett.* **109**, 167201 (2012), URL <https://link.aps.org/doi/10.1103/PhysRevLett.109.167201>.
 - [7] K. A. Ross, Y. Qiu, J. R. D. Copley, H. A. Dabkowska, and B. D. Gaulin, *Phys. Rev. Lett.* **112**, 057201 (2014), URL <https://link.aps.org/doi/10.1103/PhysRevLett.112.057201>.
 - [8] T. Yildirim, A. B. Harris, A. Aharony, and O. Entin-Wohlman, *Phys. Rev. B* **52**, 10239 (1995), URL <https://link.aps.org/doi/10.1103/PhysRevB.52.10239>.
 - [9] T. Yildirim, A. B. Harris, O. Entin-Wohlman, and A. Aharony, *Phys. Rev. Lett.* **73**, 2919 (1994), URL <https://link.aps.org/doi/10.1103/PhysRevLett.73.2919>.
 - [10] T. Yildirim, A. B. Harris, O. Entin-Wohlman, and A. Aharony, *Phys. Rev. Lett.* **72**, 3710 (1994), URL <https://link.aps.org/doi/10.1103/PhysRevLett.72.3710>.
 - [11] D. Coffey, K. S. Bedell, and S. A. Trugman, *Phys. Rev. B* **42**, 6509 (1990), URL <https://link.aps.org/doi/10.1103/PhysRevB.42.6509>.
 - [12] D. Coffey, T. M. Rice, and F. C. Zhang, *Phys. Rev. B* **44**, 10112 (1991), URL <https://link.aps.org/doi/10.1103/PhysRevB.44.10112>.
 - [13] C. J. Peters, R. J. Birgeneau, M. A. Kastner, H. Yoshizawa, Y. Endoh, J. Tranquada, G. Shirane, Y. Hidaka, M. Oda, M. Suzuki, et al., *Phys. Rev. B* **37**, 9761 (1988), URL <https://link.aps.org/doi/10.1103/PhysRevB.37.9761>.
 - [14] B. Keimer, R. J. Birgeneau, A. Cassanho, Y. Endoh, M. Greven, M. A. Kastner, and G. Shirane, *Zeitschrift für Physik B Condensed Matter* **91**, 373 (1993), ISSN 1431-584X, URL <https://doi.org/10.1007/BF01344067>.
 - [15] K. Katsumata, M. Hagiwara, Z. Honda, J. Satooka, A. Aharony, R. J. Birgeneau, F. Chou, O. Entin-Wohlman, A. Harris, M. A. Kastner, et al. (2000).
 - [16] F. C. Chou, A. Aharony, R. J. Birgeneau, O. Entin-Wohlman, M. Greven, A. B. Harris, M. A. Kastner, Y. J. Kim, D. S. Kleinberg, Y. S. Lee, et al., *Phys. Rev. Lett.* **78**, 535 (1997), URL <https://link.aps.org/doi/10.1103/PhysRevLett.78.535>.
 - [17] Y. J. Kim, A. Aharony, R. J. Birgeneau, F. C. Chou, O. Entin-Wohlman, R. W. Erwin, M. Greven, A. B. Harris, M. A. Kastner, I. Y. Korenblit, et al., *Phys. Rev. Lett.* **83**, 852 (1999), URL <https://link.aps.org/doi/10.1103/PhysRevLett.83.852>.
 - [18] P. Burlet, J. Henry, and L. Regnault, *Physica C: Superconductivity* **296**, 205 (1998), ISSN 0921-4534, URL <http://www.sciencedirect.com/science/article/pii/S0921453497018364>.
 - [19] J. L. Garcia-Munoz, J. Rodriguez-Carvajal, F. Sapina, M. J. Sanchis, R. Ibanez, and D. Beltran-Porter, *Journal of Physics: Condensed Matter* **2**, 2205 (1990), URL <http://stacks.iop.org/0953-8984/2/i=9/a=010>.
 - [20] L. Zhao, H. Guo, W. Schmidt, K. Nemkovski, M. Mostovoy, and A. C. Komarek, *Phys. Rev. B* **96**, 054424 (2017), URL <https://link.aps.org/doi/10.1103/PhysRevB.96.054424>.
 - [21] R. Troc, J. Janicki, I. Filatow, P. Fischer, and A. Murasik, *Journal of Physics: Condensed Matter* **2**, 6989 (1990), URL <http://stacks.iop.org/0953-8984/2/i=33/a=011>.
 - [22] J. Konstantinovic, G. Stanisic, M. Ain, and G. Parette, *Journal of Physics: Condensed Matter* **3**, 381 (1991), URL <http://stacks.iop.org/0953-8984/3/i=3/a=014>.
 - [23] K. Yamada, K. ichi Takada, S. Hosoya, Y. Watanabe, Y. Endoh, N. Tomonaga, T. Suzuki, T. Ishigaki, T. Kamiyama, H. Asano, et al., *Journal of the Physical Society of Japan* **60**, 2406 (1991), <https://doi.org/10.1143/JPSJ.60.2406>, URL <https://doi.org/10.1143/JPSJ.60.2406>.
 - [24] M. Ain, G. Dhalenne, O. Guiselin, B. Hennion, and A. Revcolevschi, *Phys. Rev. B* **47**, 8167 (1993), URL <https://link.aps.org/doi/10.1103/PhysRevB.47.8167>.
 - [25] T. Moriya, *Phys. Rev.* **120**, 91 (1960), URL <https://link.aps.org/doi/10.1103/PhysRev.120.91>.
 - [26] B. Roessli, P. Fischer, A. Furrer, G. Petrakovskii, K. Sablina, V. Valkov, and B. Fedoseev, *Journal of Applied Physics* **73**, 6448 (1993), <https://doi.org/10.1063/1.352629>, URL <https://doi.org/10.1063/1.352629>.
 - [27] O. Janson, R. O. Kuzian, S.-L. Drechsler, and H. Rosner, *Phys. Rev. B* **76**, 115119 (2007), URL <https://link.aps.org/doi/10.1103/PhysRevB.76.115119>.
 - [28] B. Roessli, B. Fk, M.-T. Fernandez-Daz, K. Sablina, and G. Petrakovskii, *Physica B: Condensed Matter* **234-236**, 726 (1997), ISSN 0921-4526, proceedings of the First European Conference on Neutron Scattering, URL <http://www.sciencedirect.com/science/article/pii/S0921452696011295>.
 - [29] H. Ohta, Y. Ikeuchi, S. Kimura, S. Okubo, H. Nojiri, M. Motokawa, S. Hosoya, K. Yamada, and Y. Endoh, *Physica B: Condensed Matter* **246-247**, 557 (1998), ISSN 0921-4526, URL <http://www.sciencedirect.com/science/article/pii/S0921452697009861>.